

# Inhibitory Effects of Glucosamine on Endotoxin-Induced Uveitis in Lewis Rats

Yun-Hsiang Chang,<sup>1</sup> Chi-Ting Horng,<sup>2,3</sup> Yi-Hao Chen,<sup>1</sup> Po-Liang Chen,<sup>1</sup> Ching-Long Chen,<sup>1</sup> Chang-Min Liang,<sup>4</sup> Ming-Wei Chien,<sup>4</sup> and Jiann-Torng Chen<sup>1,4</sup>

**PURPOSE.** Glucosamine sulfate (GS) is a naturally occurring sugar that exerts immunosuppressive effects *in vitro* and *in vivo*. The authors investigated whether GS modulates the inflammatory reaction in endotoxin-induced uveitis (EIU) of rats and the mechanisms by which it exerts its effects.

**METHODS.** Two-hundred micrograms of lipopolysaccharide (LPS) was injected subcutaneously into Lewis rats to induce EIU. Doses of GS (10, 100, or 1000 mg/kg) were divided into three aliquots and administered intraperitoneally 30 minutes before LPS injection, concurrently with LPS injection, and 30 minutes after LPS injection. Twenty-four hours after LPS injection, aqueous humor was collected for cell counting and measurement of protein concentration. Immunohistochemical staining of the iris-ciliary body was performed to evaluate the effects of GS on intercellular adhesion molecule (ICAM)-1 and nuclear factor (NF)- $\kappa$ B activation and to demonstrate macrophage infiltration. The effects of various doses of GS pretreatment were also examined using a mouse macrophage cell line (RAW264.7 cells) and LPS stimulation. Levels of prostaglandin (PG)-E2 and nitric oxide (NO) were determined. Expression of inducible NO synthase (iNOS) and cyclooxygenase (COX)-2 were measured using Western blot analysis. The effect of GS on LPS-induced NF- $\kappa$ B activation in RAW cells was also examined.

**RESULTS.** Cell counting and analysis of protein concentration in aqueous humor revealed that GS suppressed EIU in rats treated with a high dose of GS (1000 mg/kg). Immunohistochemistry showed that treatment with GS reduced ICAM-1 expression and suppressed activation of NF- $\kappa$ B in the iris-ciliary body. The main inflammatory cells in the iris-ciliary body during EIU were macrophages. In LPS-stimulated macrophage RAW cell culture, GS inhibited the production of NO and PG-E2, the expression of iNOS and COX-2, and the activation of NF- $\kappa$ B.

**CONCLUSIONS.** GS suppresses EIU in rats by blocking the NF- $\kappa$ B-dependent signaling pathway and the subsequent production of ICAM-1 and proinflammatory mediators. This study has extended the authors' previous observation that GS is a potentially important compound for reducing ICAM-1-mediated inflammatory effects in the eye. (*Invest Ophthalmol Vis Sci.* 2008;49:5441-5449) DOI:10.1167/iovs.08-1784

Endotoxin-induced uveitis (EIU) is an acute form of uveitis that can be induced by giving rats,<sup>1</sup> mice,<sup>2</sup> and rabbits<sup>3</sup> systemic injections of a sublethal dose of lipopolysaccharide (LPS), a component of the cell walls of Gram-negative bacteria. Symptoms of EIU usually manifest 4 hours after LPS injection, peak at 18 to 24 hours after LPS injection, and persist for 72 hours. The histopathology of EIU is characterized by transient but intense acute cellular infiltration of the anterior and posterior segments of the eye by neutrophils and macrophages. Although the pathogenesis of EIU is unclear, it is known that proinflammatory cytokines such as tumor necrosis factor (TNF)- $\alpha$ , interleukin (IL)-1 $\beta$ , interferon (INF)- $\gamma$ , and IL-6,<sup>4-7</sup> inflammatory mediators such as nitric oxide (NO)<sup>8</sup> and prostaglandin (PG)-E2,<sup>9</sup> and cell-adhesion molecules such as intercellular adhesion molecule (ICAM)-1<sup>10</sup> are involved.

The production and release of inflammatory mediators and adhesion molecules in response to LPS is dependent on inducible gene expression, which is mediated by the activation of transcription factors such as NF- $\kappa$ B. Inactive NF- $\kappa$ B is a heterodimer of p50 and p65 (RelA); it is present in the cytoplasm and is sequestered by the inhibitor of kappa B (I $\kappa$ B) family of inhibitors.<sup>11,12</sup> After the phosphorylation and degradation of I $\kappa$ B, the p50-p65 component is released and translocates to the nucleus, where it activates the transcription of genes involved in innate immunity, inflammation, and cell survival.<sup>13-15</sup>

An *in vitro* study has shown that monosaccharides, especially those with amino groups, can inhibit cytotoxic T-lymphocyte activity.<sup>16</sup> Moreover, hexosamines inhibit natural killer cell cytotoxicity.<sup>17</sup> Glucosamine sulfate (GS), a naturally occurring hexosamine, exerts immunosuppressive effects *in vitro* and *in vivo*.<sup>18,19</sup> It prolongs cardiac allograft survival *in vivo* by suppressing the activation of T-lymphoblasts and dendritic cells.<sup>18</sup> GS also augments type II decoy receptor expression and suppresses NF- $\kappa$ B activity and IL-1 $\beta$  bioactivity in rat chondrocytes.<sup>19</sup> We recently demonstrated that GS suppresses ICAM-1 expression and leukocyte adhesion induced by proinflammatory cytokine stimulation of retinal pigment epithelial cells and conjunctival cells *in vitro*.<sup>20-22</sup> These results stimulated us to investigate the effect of GS on EIU, an animal model of uveitis.

The purpose of our study was to investigate the effects of GS on EIU in rats. We found that GS inhibited LPS-induced cellular infiltration and protein leakage in aqueous humor. To elucidate the mechanisms responsible for the anti-inflammatory effects of GS, we investigated the expression of ICAM-1 and the activation of NF- $\kappa$ B in the iris-ciliary body and found that both were suppressed by GS. We also demonstrated that GS inhibits the production of NO and PG-E2 and the expression of inducible NO synthase (iNOS) and cyclooxygenase (COX)-2

From the <sup>1</sup>Department of Ophthalmology, Tri-Service General Hospital, Taipei, Taiwan, Republic of China; the <sup>2</sup>Department of Ophthalmology, Kaohsiung Armed Force General Hospital, Kaohsiung, Taiwan, Republic of China; the <sup>3</sup>Department of Pharmacy, Tajen University, Pintung, Taiwan, Republic of China; and the <sup>4</sup>Department of Ophthalmology, National Defense Medical Center, Taipei, Taiwan, Republic of China.

Supported in part by Grants TSGH-C96-6-S01, TSGH-C96-6-S02, TSGH-C96-6-S03, and TSGH-C96-6-S04 from the Tri-Service General Hospital and Grant NSC-96-2314-B-016-021-MY3 from the National Science Council.

Submitted for publication January 23, 2008; revised June 16 and August 6, 2008; accepted October 8, 2008.

Disclosure: Y.-H. Chang, None; C.-T. Horng, None; Y.-H. Chen, None; P.-L. Chen, None; C.-L. Chen, None; C.-M. Liang, None; M.-W. Chien, None; J.-T. Chen, None

The publication costs of this article were defrayed in part by page charge payment. This article must therefore be marked "advertisement" in accordance with 18 U.S.C. §1734 solely to indicate this fact.

Corresponding author: Jiann-Torng Chen, Department of Ophthalmology, Tri-Service General Hospital, National Defense Medical Center, 325, Cheng-Kung Road, Section 2, Taipei, Taiwan, Republic of China; jt66chen@ms32.hinet.net.

in LPS-stimulated RAW 264.7 cells. Activation of NF- $\kappa$ B by LPS in RAW cells was also suppressed by GS.

## METHODS

### Animals and Induction of EIU

Eight-week-old male Lewis rats (210–220 g) were used in this study. They were maintained under a 12-hour light/12-hour dark cycle. Food and water were supplied ad libitum. All the animals were cared for in accordance with the ARVO Statement for the Use of Animals in Ophthalmic and Vision Research.

Rats were randomly allocated to a control group or a treatment group that was subdivided into an LPS group, a GS group, and an LPS + GS group. There were 12 rats in each group. Eight of the 12 rats were used for the collection of aqueous humor; one eye was used for cell counting and the other for the protein concentration assay. The other four rats were used for immunohistologic analysis. To induce EIU, 200  $\mu$ g LPS from *Salmonella typhimurium* (Sigma-Aldrich, St. Louis, MO) that had been diluted in 0.2 mL phosphate-buffered saline (PBS; pH 7.4) was injected into one footpad of each rat of the LPS and the LPS + GS groups. In the GS and LPS + GS groups, rats were injected intraperitoneally with 10, 100, or 1000 mg/kg GS (Sigma-Aldrich) divided into three aliquots administered 30 minutes before LPS injection, simultaneously with LPS injection, and 30 minutes after LPS injection. This sequence of GS injections was used because of the pharmacokinetics of glucosamine.<sup>23</sup> In the LPS group, 0.5 mL PBS was administered intraperitoneally using the schedule described for GS injection in the GS and LPS + GS groups. In the control group, neither LPS nor GS was injected into the rats; they received only vehicle. Rats were humanely killed 24 hours after LPS injection.

### Cell Counts and Protein Concentration

Immediately after euthanatization, aqueous humor was collected by puncture of the anterior chamber of the eye with a 30-gauge needle. For cell counting, the aqueous humor was mixed with an equal amount of trypan blue solution (Sigma-Aldrich), and 1 drop of the cell suspension was applied to a hemocytometer. The number of cells per square (equivalent to 0.1  $\mu$ L) was counted manually using a light microscope, and the mean number of counts from five squares per sample was multiplied by 2 to correct the previous dilution.

Total protein concentration in aqueous humor was measured using a BCA protein assay reagent kit (Pierce, Rockford, IL).

### Histology and Immunohistology

For histology and immunohistology, eyes were enucleated immediately after death and immersed in 4% paraformaldehyde for at least 24 hours, after which they were snap-frozen in liquid nitrogen and embedded in OCT compound in cryomolds. More than 20 serial axial cryostat sections (6- $\mu$ m thick) were cut from each eye, starting at the optic nerve head.

Sections were stained with hematoxylin and eosin for histology. For immunohistology, sections were incubated with anti-ICAM-1 antibody (1A29, dilution 1:50; Chemicon, Temecula, CA), anti-macrophage subset antibody (HIS36, dilution 1:50; Santa Cruz Biotechnology, Santa Cruz, CA), or anti-NF- $\kappa$ B p65 antibody (C20, sc-372, dilution 1:50; Santa Cruz Biotechnology) overnight at 4°C. Sections were blocked with 5% fetal bovine serum (heat inactivated, no. 26140; Invitrogen, Carlsbad, CA). Tissues were then probed with a fluorescein isothiocyanate (FITC)-labeled secondary antibody (1:50 dilution; Jackson ImmunoResearch Laboratories, West Grove, PA). Cells were also stained with 4', 6-diamidino-2-phenylindole (DAPI; Sigma-Aldrich) for 5 minutes for localization and quantification of nuclei. Preparations were mounted in 70% glycerol and were examined using fluorescence microscopy. The same exposure was used for photographing all samples, and the nuclei were quantified using the images.

### NF- $\kappa$ B p65 Nuclear Translocation

To calculate the percentage of NF- $\kappa$ B-positive cells in the iris-ciliary body, four intact sections from each eye, of equal length and 30  $\mu$ m apart from each other, were evaluated. After immunostaining for NF- $\kappa$ B p65, the two iris-ciliary bodies appearing on each slide were photographed. The total number of cells and the number of NF- $\kappa$ B-positive cells that had translocated to the nuclei in the photograph were counted manually by an investigator who was masked to the treatment samples. The number of NF- $\kappa$ B-positive cells was expressed as a percentage of the total number of cells present. The mean number of NF- $\kappa$ B-positive cells per rat was calculated from four slides per eye from both eyes. Group means were calculated from four rats per group.

### Cell Culture and Treatment

Mouse macrophage-like RAW264.7 cells were obtained from the Bioresource Collection and Research Center (Taipei, Taiwan) and were grown in Dulbecco modified Eagle medium (DMEM) supplemented with 4 mM L-glutamine, 10% FBS, 100 U/mL penicillin, and 100 mg/mL streptomycin at 37°C in an atmosphere containing 5% CO<sub>2</sub>.

In each experiment, the RAW264.7 cells were preincubated with GS (Sigma-Aldrich), glucose (Glu; Sigma-Aldrich), N-acetylglucosamine (N-AcG; Sigma-Aldrich), or galactosamine hydrochloride (Gal; Sigma-Aldrich) at the indicated concentration for 2 hours and were then stimulated for 24 hours with 1  $\mu$ g/mL LPS (Sigma-Aldrich) derived from *S. typhimurium*.

### Western Blotting

RAW264.7 cells were scraped from the culture dishes and lysed in 2 $\times$  sample buffer. The samples were boiled for 10 minutes, electrophoresed using 10% SDS-PAGE, and transferred to polyvinylidene difluoride membranes (Immobilion; Millipore, Bedford, MA). Blots were probed with 1:1000 dilutions of anti-iNOS (06-573; Upstate Biotechnology, Lake Placid, NY) or anti-COX-2 (C-20; Santa Cruz Biotechnology) for 1 hour at room temperature and were then washed three times with TBST buffer. After incubation with a horseradish peroxidase-conjugated secondary antibody (Jackson ImmunoResearch Laboratories) for 1 hour at room temperature, blots were washed three times and developed using an enhanced chemiluminescence system (Millipore). The densities and areas of spots on the developed images were measured. Four independent repetitions of each experiment were performed.

### Measurement of NO and PG-E2 Concentrations

Concentrations of NO and PG-E2 in cell cultures were measured using a NO quantitation kit (Active Motif, Carlsbad, CA) and a PG-E2 ELISA kit (Neogen, Lansing, MI), respectively. Four independent repetitions of each experiment were performed.

### Immunofluorescence Staining

RAW264.7 cells with or without GS pretreatment were incubated with 1  $\mu$ g/mL LPS for 60 minutes. After incubation, cells were washed, fixed in methanol/acetone (1:1) for 1 hour at -20°C, and treated with 0.1% Triton X-100 for 10 minutes on ice. Cells were further incubated in PBS containing 5% BSA for 1 hour at room temperature to counter nonspecific binding of the primary antibody. Rabbit polyclonal antibodies against p65 (1:200 dilution; Santa Cruz Biotechnology) were used as primary antibodies. FITC-labeled goat anti-rabbit IgG (1:200 dilution; Jackson ImmunoResearch) was used as the secondary antibody. Cells were examined using fluorescence microscopy. The same exposure was used for photographing all samples.

### Statistical Analysis

Student's *t*-test was used for comparisons involving two group means. One-way analysis of variance (ANOVA) and the Bonferroni test were used for comparisons involving three or more group means. Data are

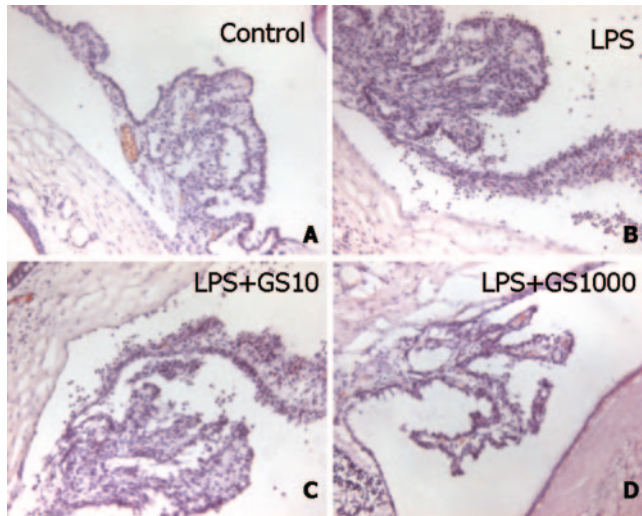


**FIGURE 1.** Histopathologic features of inflammatory cell infiltration in the iris-ciliary bodies of rats in the (A) control group and in treatment groups (B) LPS, (C) LPS + 10 mg/kg GS, and (D) LPS + 1000 mg/kg GS. There was no cellular infiltration in the control group (A), but severe inflammatory cell infiltration was evident in the LPS group (B). The suppressive effect of GS on cellular infiltration was dose dependent in the LPS + GS group (compare C with D). Original magnification,  $\times 200$ .

expressed as mean  $\pm$  SEM.  $P \leq 0.05$  was considered statistically significant.

## RESULTS

### Histopathology of the Effect of GS on EIU

Twenty-four hours after LPS injection, severe cellular infiltration was observed in the iris-ciliary bodies of the LPS group (Fig. 1B) and in the LPS + GS subgroups treated with low doses of GS (10 and 100 mg/kg GS; Fig. 1C). A significant reduction of cellular infiltration was observed in the anterior segment of LPS + GS rats treated with 1000 mg/kg GS (Fig. 1D). There was no cellular infiltration in the iris-ciliary body in the control group (Fig. 1A) and the GS group (data not shown).

### Effect of GS on Cellular Infiltration and Protein Concentration of Aqueous Humor

Twenty-four hours after LPS administration, the aqueous humor of the LPS group contained  $96.65 \pm 8.45 \times 10^5$ /mL inflammatory cells ( $n = 8$ ). When treated with GS at a dose of 1000 mg/kg, the concentration of inflammatory cells 24 hours after the administration of LPS was significantly lower ( $15.9 \pm 3.70 \times 10^5$ /mL;  $P < 0.01$ ) than that in the LPS group. The levels of inflammatory cells 24 hours after the administration of LPS in rats treated with GS doses of 10 mg/kg and 100 mg/kg ( $91.90 \pm 12.99 \times 10^5$ /mL and  $87.32 \pm 12.28 \times 10^5$ /mL, respectively) were slightly lower than those of the LPS group, but the differences were not significant (Fig. 2A). There were few inflammatory cells in the anterior segments of rats in the control and GS groups.

The concentration of protein in aqueous humor was substantially greater in the LPS group than in the control and GS groups. In the LPS + GS group, a reduction in protein concentrations was observed with low-dose GS treatments (10 and 100 mg/kg), but the effects were not significant. The protein concentration was significantly reduced only by the high dose of GS (1000 mg/kg; Fig. 2B).

### Effect of GS on ICAM-1 Expression in the Iris-Ciliary Body of EIU Rats

Given that ICAM-1 plays a key role in leukocyte adhesion and infiltration, we determined whether GS affects ICAM-1 expression in the iris-ciliary body. The iris-ciliary body constitutively expressed low levels of ICAM-1, as determined by immunohistochemistry (Fig. 3A). Strong expression of ICAM-1 in the iris-ciliary body was evident 24 hours after LPS injection (Fig. 3C). Rats in the LPS + GS subgroup that received a GS dose of 1000 mg/kg showed a marked decrease in ICAM-1 expression 24 hours after LPS administration (Fig. 3G).

### Effect of GS on NF- $\kappa$ B Activation in the Iris-Ciliary Body of EIU Rats

NF- $\kappa$ B is composed of two groups of structurally related interactive proteins that bind to DNA recognition sites as a dimer whose activity is regulated by its subcellular location.<sup>24</sup> Because NF- $\kappa$ B activity is essential for the activation of endotoxin-induced ICAM-1 expression,<sup>25,26</sup> we used an immunofluorescence assay to examine the location of the p65 subunit of NF- $\kappa$ B within the iris-ciliary body. Figure 4A shows that there was little activated NF- $\kappa$ B p65 in the iris-ciliary body in the control and GS groups. In rats injected with LPS, nuclear translocation of the activated NF- $\kappa$ B p65 subunit was observed. Activation was decreased by the addition of GS in the LPS + GS group (Fig. 4A). Quantitative analysis of cells positive for NF- $\kappa$ B revealed that LPS-induced NF- $\kappa$ B activation was suppressed by GS in a dose-dependent manner (Fig. 4B).

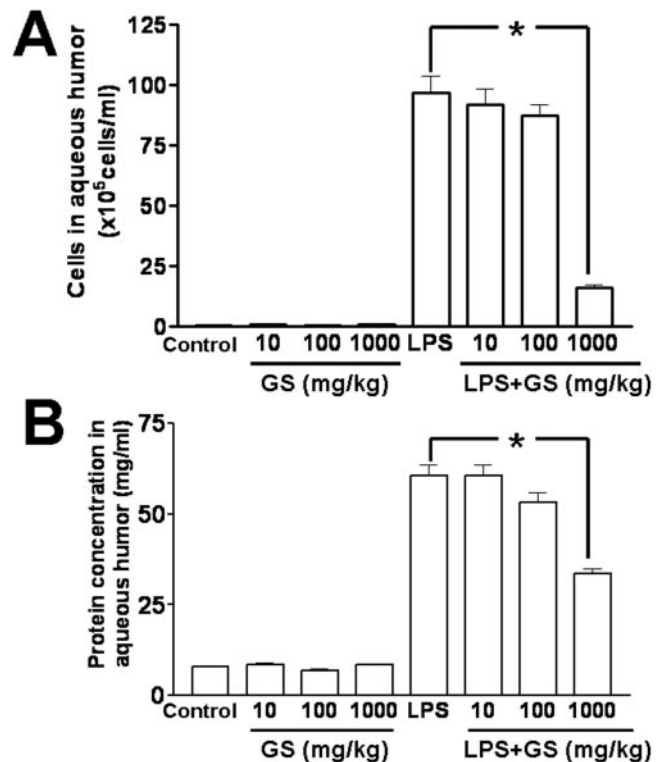


**FIGURE 2.** Effects of GS on (A) cellular infiltration and (B) protein concentration in aqueous humor 24 hours after LPS injection. Note that GS had no effect on basal (unstimulated) rates of cellular infiltration and protein concentration. LPS stimulation markedly increased cell count and protein concentration, which were significantly suppressed by the high-dose GS treatment (1000 mg/kg). Means were derived from eight rats. \*Significantly different from the LPS group.

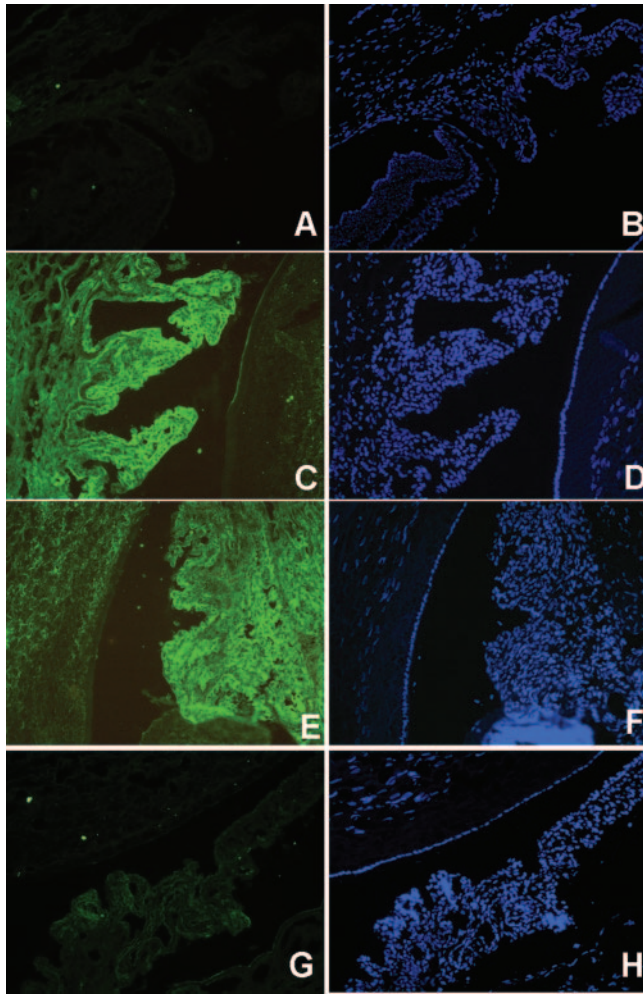


**FIGURE 3.** Immunofluorescence images showing the effect of GS on LPS-induced ICAM-1 expression in the iris-ciliary body of rats. (A, C, E, G) Sections stained with antibody against ICAM-1. (B, D, F, H) Sections stained with DAPI for the localization of nuclei. (A, B) Control groups, which received neither LPS nor GS. (C, D) LPS group (rats were injected with LPS). (E, F) LPS + GS group (rats were injected with LPS and 10 mg/kg GS). (G, H) LPS + GS group (rats were injected with LPS and 1000 mg/kg GS). Original magnification,  $\times 200$ .

### ED2-like Antigen Expression in Inflammatory Cells in the Iris-Ciliary Body

ED2-like antigen is a macrophage-specific antigen. To determine whether macrophages participate in the cellular infiltration into the anterior chamber and the iris-ciliary body during EIU, we used immunofluorescence to stain samples from the LPS group and the LPS + GS group for ED2-like antigen. Most cells that infiltrated the anterior chamber and iris-ciliary body were positive for ED2-like antigen (Fig. 5).

### Effects of GS on Expression of COX-2 and iNOS and Levels of PG-E2 and NO

To investigate whether GS affects the COX-2-PG-E2 and iNOS-NO pathways, we assessed changes in the levels of COX-2, PG-E2, iNOS, and NO before and after administration of LPS to RAW cells that had been subjected to GS preincubation or had not been exposed to GS. Trace amounts of iNOS and COX-2 were detected in vehicle-treated and GS-treated cells. After 24 hours of culture, unstimulated macrophages expressed background levels of iNOS (Fig. 6A) and COX-2 (Fig.

6B). When the RAW cells were incubated with GS alone, iNOS and COX-2 in the medium were maintained at concentrations similar to those of unstimulated samples. After treatment with LPS (1  $\mu\text{g}/\text{mL}$ ) for 24 hours, iNOS and COX-2 concentrations increased by 25-fold and 22-fold, respectively. When macrophages were incubated with various concentrations of GS (0.046, 0.46, or 4.6 mM) together with 1  $\mu\text{g}/\text{mL}$  LPS for 24 hours, significant concentration-dependent inhibition of iNOS and COX-2 expression was observed, as was the case with NO (Fig. 7A) and PG-E2 (Fig. 7B). Trace amounts of NO and PG-E2 were detected in unstimulated and GS-treated RAW cells. After 24 hours of LPS treatment, the production of NO increased 1.9-fold, and the concentration of PG-E2 increased to 4.9 ng/mL. Preincubation with GS suppressed LPS-induced NO and PG-E2 production in a dose-dependent manner. RAW264.7 cell viability, determined with the use of the MTT assay, was not affected by the addition of GS at a dose of 4.6 mM (data not shown).

### Effects of Different Hexosamines on iNOS, COX-2, NO, and PGE2 Levels Induced with LPS

To study whether other hexosamines also inhibit LPS-induced iNOS, COX-2, NO, and PGE2 expression, we incubated RAW cells with equimolar concentrations (4.6 mM) of GS, Glu, N-AcG, or Gal for 2 hours before stimulation with LPS for 24 hours. GS significantly reduced LPS-induced iNOS, COX-2 (Figs. 6C, 6D), NO, and PGE2 (Figs. 7C, 7D) levels. Although Glu, N-AcG, and Gal all had some inhibitory effects on iNOS and COX-2, these effects were not significant (Figs. 6C, 6D). Moreover, their effects on NO and PGE2 were not obvious (Figs. 7C, 7D).

### Immunostaining of NF- $\kappa$ B Subunit p65 in RAW Cells

To investigate the activation of NF- $\kappa$ B after LPS stimulation and the effect of GS on it in RAW cells, we performed immunofluorescence staining of NF- $\kappa$ B p65. In vehicle-treated and GS-treated cells, cytoplasmic staining with nuclear sparing was evident (Figs. 8A, 8B). Nuclear staining was evident after LPS stimulation, indicating that NF- $\kappa$ B had been activated and had translocated to the nucleus (Fig. 8C). GS pretreatment prevented nuclear staining, suggesting that activation and nuclear translocation of NF- $\kappa$ B were blocked by GS.

## DISCUSSION

We demonstrated that GS inhibits cellular infiltration and protein concentration in the aqueous humor of a rat EIU model. Immunostaining showed that LPS-induced ICAM-1 expression and NF- $\kappa$ B activation were also suppressed by GS. These results are compatible with those of our previous *in vitro* studies.<sup>20-22</sup> To investigate the mechanisms responsible for these results, we used RAW264.7 cells, a mouse macrophage cell line, as an *in vitro* model. Concentrations of iNOS, NO, COX-2, and PG-E2 were significantly lower in the LPS + GS group than in the LPS group but not in the groups treated with the control sugars, as was NF- $\kappa$ B p65 activation.

GS dosages and administration intervals used in this study were chosen for the following reasons. First, in a preliminary study, we administered a single low dosage of GS simultaneously with LPS, but it had no effect on EIU at this level (data not shown). For intraperitoneal injection of GS in rats, the LD<sub>50</sub> was 5247 mg/kg, and the rat no-observed-adverse-effect level (NOAEL) was 2700 mg/kg.<sup>27</sup> The largest dose of GS used in our study was 1000 mg/kg, which was lower than the NOAEL and was administered in thirds at intervals. Second, plasma GS levels peak at 12.5 minutes after intraperitoneal GS administra-

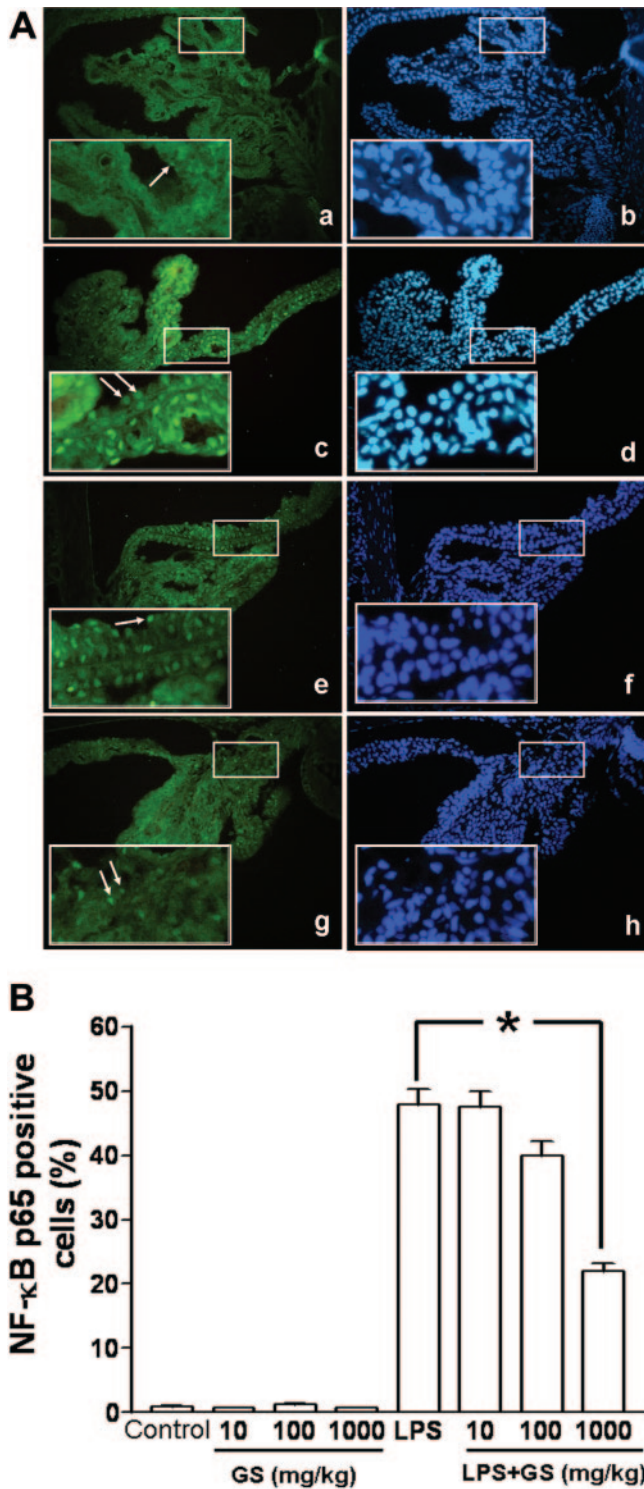


**FIGURE 4.** The effect of GS on NF-κB activation. (A) Immunohistochemistry of NF-κB p65 in the iris-ciliary body of rats. (a, c, e, g) Sections stained with antibody against p65. (b, d, f, h) Sections stained with DAPI for localization of nuclei. An area of each panel (lower left) was selected, magnified, and shown to provide better resolution. The selected area is exactly the same in the paired panels. (a, b) Control group in which neither LPS nor GS was injected. (c, d) LPS group in which rats were injected with LPS. (e, f) LPS + GS group in which rats were injected with LPS and GS (10 mg/kg). (g, h) LPS + GS group in which rats were injected with LPS and GS (1000 mg/kg). Arrows: NF-κB p65 nuclear translocation-positive cells. Original magnification, ×200. (B) Percentage of activated NF-κB p65-positive cells in the

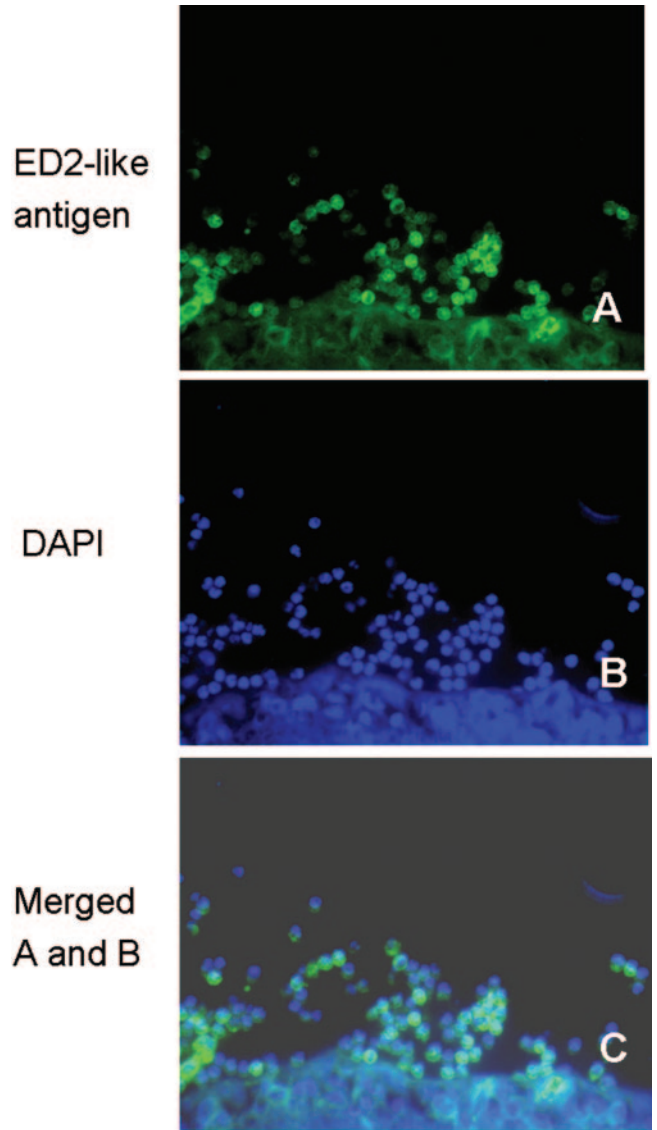


**FIGURE 5.** Double labeling of inflammatory cells in the anterior segment of a rat in the LPS group. (A) Immunostaining of macrophage-specific ED2-like antigen. (B) DAPI staining of nuclei. (C) Image obtained by merging (A) and (B) showing that the infiltrating cells were predominantly macrophages.

tion, and the half-life of GS is  $0.69 \pm 0.5$  hour.<sup>23</sup> Accordingly, to maintain high levels of GS before and after LPS injection, GS doses were administered in thirds 30 minutes before LPS injection, concurrently with LPS injection, and 30 minutes after LPS injection.

During the endotoxin-induced inflammatory reaction, the interaction between ICAM-1 and lymphocyte functional antigen (LFA)-1 is primarily responsible for the adhesion of leukocytes before extravasation.<sup>28,29</sup> In the animal model of EIU, LPS is used to induce ICAM-1 expression in the iris-ciliary body.<sup>30</sup> Because systemic administration of a monoclonal antibody against ICAM-1 has been shown to suppress LPS-induced cel-

iris-ciliary body. Mean activated NF-κB p65-positive cells in each rat were calculated from four slides per eye for both eyes. Group means were calculated from four rats per group. Values are expressed as mean ± SD (n = 4). \*Significantly different from the LPS group.

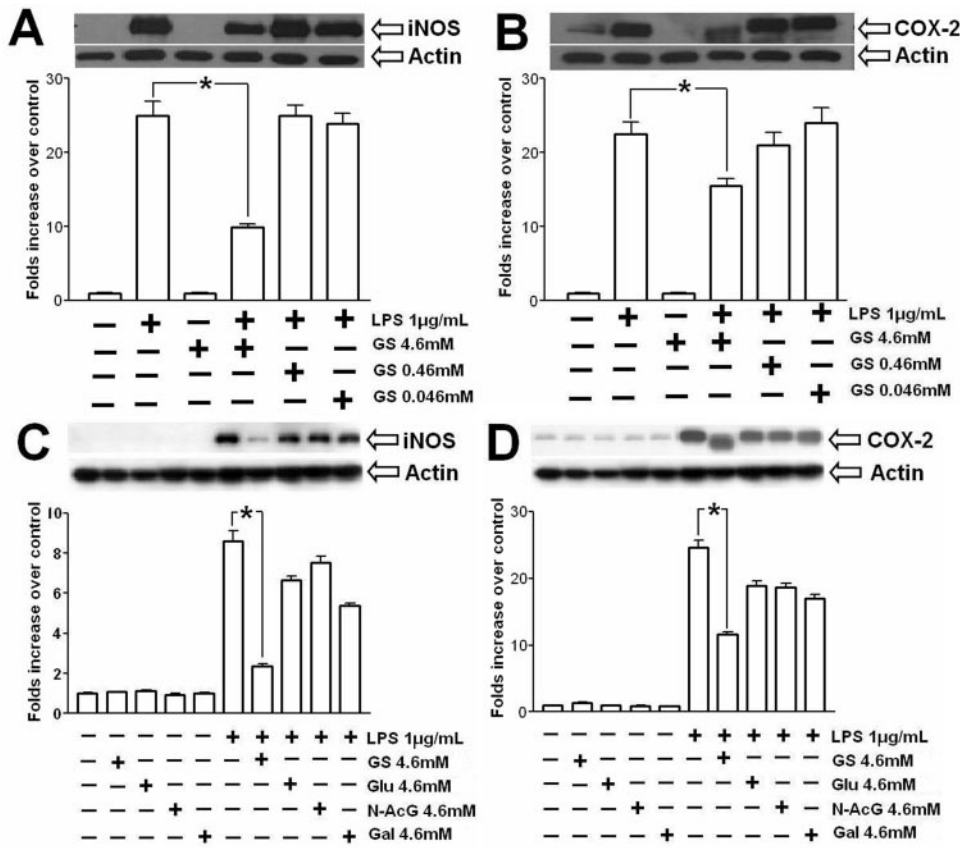


**FIGURE 6.** Effects of different concentrations of GS (A, B) and different hexosamines (C, D) on LPS-induced levels of iNOS protein and COX-2 protein in RAW cells. (A, B) RAW cells were preincubated with the indicated concentrations of GS for 2 hours and then were stimulated with 1 µg/mL LPS for 24 hours. (C, D) RAW cells were preincubated with GS, Glu, N-AcG, or Gal (4.6 mM) for 2 hours and then were stimulated with 1 µg/mL LPS for 24 hours. Protein levels were quantified by Western blot analysis and are expressed as multiples of the control mean. Data are expressed as the mean ± SEM; *n* = 4; \**P* < 0.05 compared with the LPS-treated group.

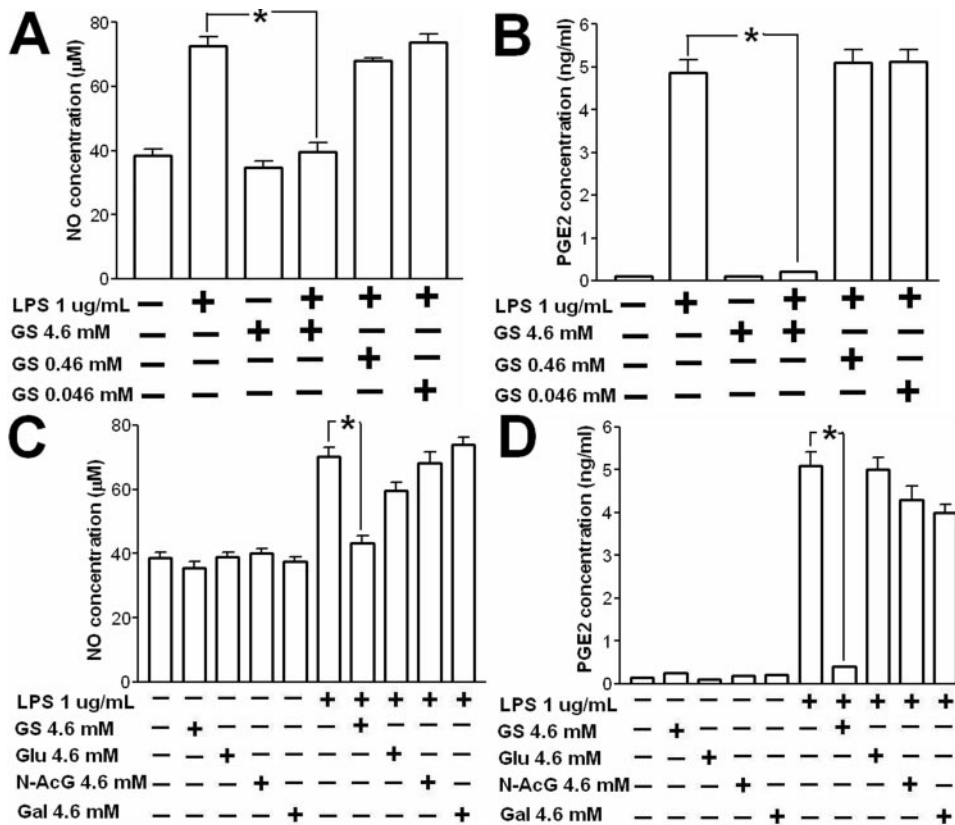


**FIGURE 7.** Effects of different concentrations of GS (A, B) and different hexosamines (C, D) on the levels of NO and PGE2 in LPS-treated RAW cells. (A, B) RAW cells were preincubated with the indicated concentrations of GS for 2 hours and then were stimulated with 1 µg/mL LPS for 24 hours. (C, D) RAW cells were preincubated with GS, Glu, N-AcG, or Gal (4.6 mM) for 2 hours and then were stimulated with 1 µg/mL LPS for 24 hours. Levels of NO and PGE2 were quantified using a commercially available NO quantitation kit and an ELISA kit, respectively. Data are expressed as mean ± SEM; *n* = 4; \**P* < 0.05 compared with the LPS-treated group.

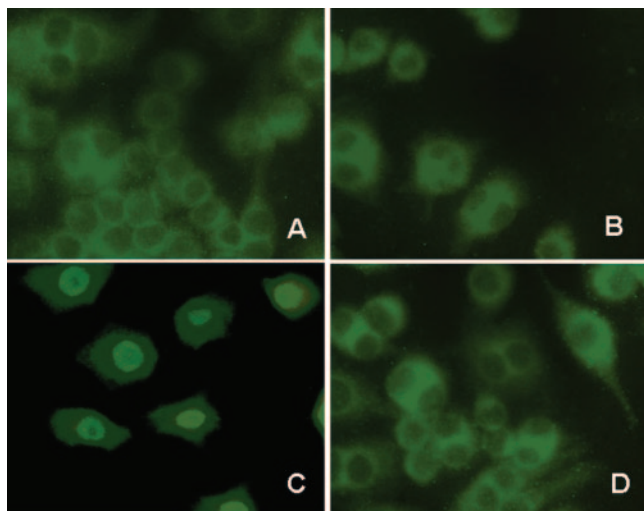


**FIGURE 8.** Immunofluorescence images of the p65 subunit of NF- $\kappa$ B in RAW cells stained with antibody against p65. (A) Immunostaining is evident in the cytoplasm of control cells but not in the nuclei. (B) Incubation with GS (4.6 mM) alone did not result in nuclear staining. (C) When RAW cells were stimulated with LPS (1  $\mu$ g/mL) for 1 hour, intense nuclear immunostaining was evident. (D) When RAW cells were pretreated with GS (4.6 mM) and then stimulated with LPS (1  $\mu$ g/mL) for 1 hour, a significant decrease in p65 nuclear immunostaining compared with LPS-treated cells was evident. Original magnification,  $\times 200$ .

lular infiltration into the anterior segment,<sup>10,31</sup> we considered that ICAM-1 may play a key role in cellular infiltration in EIU. In our previous reports, we demonstrated that proinflammatory cytokine-induced ICAM-1 gene expression and protein synthesis is inhibited by GS.<sup>20,22</sup> We also showed that in retinal pigment epithelial (RPE) cells, neutrophil adherence, which was augmented by proinflammatory cytokines, was effectively suppressed by GS.<sup>21</sup> Other authors have shown that the levels of proinflammatory cytokines we used in our previous studies (TNF- $\alpha$ , IFN- $\gamma$ , IL-1 $\beta$ , and IL-6) are elevated during EIU<sup>5</sup> and that these cytokines play important roles in the pathogenesis of EIU.<sup>4-7,32</sup> In this study, we showed that GS suppressed inflammatory cell infiltration of the aqueous humor and LPS-induced ICAM-1 expression in the iris-ciliary body in vivo. We consider this finding significant because ICAM-1 has been detected in RPE cells of patients with posterior uveitis, and elevated levels of ICAM-1 are considered to promote extravasation of inflammatory cells into the retina.<sup>33</sup> Recently, it has been demonstrated that GS suppresses the activation of T cells and dendritic cells in vitro and prolongs cardiac allograft survival in vivo.<sup>18</sup> It has been suggested that T cells, especially CD4<sup>+</sup> T cells, play an important role in EIU.<sup>2</sup> Interaction between ICAM-1 and LFA-1 serves as a costimulatory signal (signal-2) for T-cell activation, which is essential for T-cell migration to target tissues.<sup>34</sup> GS may suppress T-cell activation and the subsequent recruitment of inflammatory cells by inhibiting the interaction between ICAM-1 and LFA-1.

NF- $\kappa$ B is a heterodimer consisting mainly of p65 (RelA) and p50 and is located in the cytoplasm, where it has been associated with several inhibitory molecules.<sup>11,24,35,36</sup> Once cells are exposed to proinflammatory cytokines or endotoxin, signal transduction results in the phosphorylation and degradation of I $\kappa$ B. NF- $\kappa$ B is then released from the inhibitory signalosome, translocates to the nucleus, and induces the transcription of a variety of genes, resulting in the expression of inflammatory proteins such as ICAM-1, iNOS, and COX-2.<sup>37</sup> In our previous studies, we demonstrated that GS reduces proinflammatory cytokine-induced ICAM-1 gene expression and protein syn-

thesis in human RPE cells by preventing I $\kappa$ B degradation and thus translocation of the p65 subunit of NF- $\kappa$ B into the nucleus.<sup>20-22</sup> We now show that GS treatment dose dependently prevents LPS-induced nuclear translocation of the p65 subunit of NF- $\kappa$ B in vivo and in vitro. Taken together, these results indicate that GS exerts its anti-inflammatory effect, at least in part, by preventing nuclear translocation of the p65 subunit of NF- $\kappa$ B.

Monocytes and macrophages, which are associated with innate immunity, play an important role in the inflammatory reaction that occurs within a few hours of an LPS challenge.<sup>38</sup> IL-13, an anti-inflammatory cytokine, is secreted by T-helper-2 (Th-2) lymphocytes<sup>39</sup> and inhibits the production of proinflammatory cytokines in LPS-activated monocytes and macrophages.<sup>40-43</sup> That EIU is inhibited by intraocularly injected IL-13<sup>44</sup> suggests that activated monocytes and macrophages play a role in the pathogenesis of EIU. During EIU, macrophages in the retina and vitreous humor produce substantial amounts of NO.<sup>8</sup> Yang<sup>45</sup> found that after LPS injection, the eye undergoes a massive influx of macrophages. That finding is compatible with our finding that a major part of the inflammatory cells that infiltrated the iris-ciliary body and the anterior chamber were ED2-like antigen-positive macrophages. Accordingly, we postulated that the mouse macrophage cell line RAW 264.7 would be an ideal in vitro model for investigating the dynamics of inflammatory mediators after LPS stimulation and the effects of GS treatment.

To elucidate the mechanism responsible for the anti-inflammatory effect of GS, we evaluated the effects of GS on LPS-induced levels of proinflammatory mediators such as NO and PG-E2 and their enzymes, iNOS and COX-2, in RAW cells. Glucose, N-acetylglucosamine, and galactosamine were used as control hexosamines, and their effects on LPS-induced iNOS, COX-2, NO, and PGE2 levels were less significant than those of GS. NO is a free radical. When iNOS is induced by LPS or cytokines, NO is synthesized in large quantities by endothelial cells, macrophages, and polymorphonuclear leukocytes, resulting in protein leakage and changes in hemodynamics and vascular permeability, which are typical of EIU.<sup>46-48</sup> During EIU, the level of iNOS mRNA increases in the iris-ciliary body and the retina.<sup>49</sup> EIU can be suppressed by inhibiting the expression of iNOS,<sup>46,49,50</sup> suggesting that iNOS activation and the subsequent production of large quantities of NO contribute to the pathogenesis of EIU. On the other hand, expression of COX-2 is also induced by LPS in various tissue preparations.<sup>51-53</sup> This enzyme plays a major role in the inflammatory process by catalyzing the production of prostaglandins.<sup>54,55</sup> PG-E2 is an inflammatory mediator that causes the breakdown of the blood-aqueous barrier during EIU.<sup>56</sup> We found that LPS-induced iNOS and COX-2 expression and NO and PG-E2 production in RAW cells were suppressed by GS in a dose-dependent manner. We also showed that GS suppressed the activation of LPS-induced NF- $\kappa$ B in RAW cells. Given that the expression of iNOS and COX-2 is regulated by NF- $\kappa$ B,<sup>57,58</sup> our results indicate that GS inhibits NO and PG-E2 production by blocking NF- $\kappa$ B activation and, consequently, iNOS and COX-2 protein production. Inhibition of NO and PG-E2 has therapeutic effects on uveitis.<sup>9</sup> Given that the effects of these pathways are additive in endotoxin-induced uveitis, GS-mediated inhibition of both the iNOS/NO and the COX-2/PGE2 pathways, as observed in our study, indicates that GS administration may be a potent means of treating uveitis.

Dietary supplementation with GS is commonly used to relieve the symptoms of osteoarthritis (OA).<sup>59-62</sup> The therapeutic value of GS has been validated by several in vitro studies. It has been demonstrated that GS downregulates IL-1-induced COX-2 gene expression and subsequent PGE2 synthesis in chondrocytes and that it decreases neutrophil function

and immune activity in synovial tissue.<sup>18,63,64</sup> It has also been proposed that GS may quench small bioactive molecules such as NO and oxygen radicals, which damage articular cartilage.<sup>65</sup> In addition to the anti-inflammatory effects of GS on OA, GS may increase intracellular concentrations of UDP-N-AcG, which is essential for the formation of glycosaminoglycan, a component of cartilage.<sup>66</sup> GS is safe, and side effects in humans are rare and, if present, mild. The recommended oral dosage of GS is 1500 mg/d, which is equivalent to 25 mg/kg/d for a 60-kg adult. Doses of as much as 322.5 mg/kg (administered as a 5  $\mu$ mol/min/kg intravenous infusion over 300 minutes) have been safely administered to humans.<sup>67</sup>

In summary, this study showed that GS has dose-dependent anti-inflammatory effects on EIU in rats. Possible mechanisms for the anti-inflammatory effect of GS are suppression of the production of ICAM-1, PG-E2, and NO and inhibition of the expression of COX-2 and iNOS, which are mediated by suppression of NF- $\kappa$ B activation. Compared with the adverse effects of corticosteroids and nonsteroidal anti-inflammatory drugs, the absence of such effects with GS is attractive. However, because of its short half-life and the high intravenous dose required for GS to affect EIU in rats, its value in the treatment of uveitis requires further study.

## References

- Rosenbaum JT, McDevitt HO, Guss RB, Egbert PR. Endotoxin-induced uveitis in rats as a model for human disease. *Nature*. 1980;286(5773):611-613.
- Kogiso M, Tanouchi Y, Mimura Y, et al. Endotoxin-induced uveitis in mice, I: Induction of uveitis and role of T lymphocytes. *Jpn J Ophthalmol*. 1992;36(3):281-290.
- Howes EL Jr, Aronson SB, McKay DG. Ocular vascular permeability: effect of systemic administration of bacterial endotoxin. *Arch Ophthalmol*. 1970;84(3):360-367.
- Yoshida M, Yoshimura N, Hangai M, et al. Interleukin-1 alpha, interleukin-1 beta, and tumor necrosis factor gene expression in endotoxin-induced uveitis. *Invest Ophthalmol Vis Sci*. 1994;35(3):1107-1113.
- de Vos AF, Klaren VN, Kijlstra A. Expression of multiple cytokines and IL-1RA in the uvea and retina during endotoxin-induced uveitis in the rat. *Invest Ophthalmol Vis Sci*. 1994;35(11):3873-3883.
- de Vos AF, van Haren MA, Verhagen C, et al. Kinetics of intraocular tumor necrosis factor and interleukin-6 in endotoxin-induced uveitis in the rat. *Invest Ophthalmol Vis Sci*. 1994;35(3):1100-1106.
- Avunduk MC, Avunduk AM, Oztekin E, et al. Etanercept treatment in the endotoxin-induced uveitis of rats. *Exp Eye Res*. 2004;79(3):357-365.
- Jacquemin E, de Kozak Y, Thillaye B, et al. Expression of inducible nitric oxide synthase in the eye from endotoxin-induced uveitis rats. *Invest Ophthalmol Vis Sci*. 1996;37(6):1187-1196.
- Bellot JL, Palmero M, Garcia-Cabanes C, et al. Additive effect of nitric oxide and prostaglandin-E2 synthesis inhibitors in endotoxin-induced uveitis in the rabbit. *Inflamm Res*. 1996;45(4):203-208.
- Becker MD, Garman K, Whitcup SM, et al. Inhibition of leukocyte sticking and infiltration, but not rolling, by antibodies to ICAM-1 and LFA-1 in murine endotoxin-induced uveitis. *Invest Ophthalmol Vis Sci*. 2001;42(11):2563-2566.
- Baldwin AS Jr. The NF-kappa B and I kappa B proteins: new discoveries and insights. *Annu Rev Immunol*. 1996;14:649-683.
- Shishodia S, Aggarwal BB. Nuclear factor- $\kappa$ B: a friend or a foe in cancer? *Biochem Pharmacol*. 2004;68(6):1071-1080.
- Li X, Stark GR. NF $\kappa$ B-dependent signaling pathways. *Exp Hematol*. 2002;30(4):285-296.
- Karin M, Lin A. NF- $\kappa$ B at the crossroads of life and death. *Nat Immunol*. 2002;3(3):221-227.
- Bonizzi G, Karin M. The two NF- $\kappa$ B activation pathways and their role in innate and adaptive immunity. *Trends Immunol*. 2004;25(6):280-288.
- O'Neill HC, Parish CR. Monosaccharide inhibition of cytotoxic T-cell function: demonstration of clone-specific effects. *Immunology*. 1988;64(1):181-184.
- Yagita M, Nakajima M, Saksela E. Suppression of human natural killer cell activity by amino sugars. *Cell Immunol*. 1989;122(1):83-95.
- Ma L, Rudert WA, Harnaha J, et al. Immunosuppressive effects of glucosamine. *J Biol Chem*. 2002;277(42):39343-39349.
- Gouze JN, Bianchi A, Becuwe P, et al. Glucosamine modulates IL-1-induced activation of rat chondrocytes at a receptor level, and by inhibiting the NF-kappa B pathway. *FEBS Lett*. 2002;510(3):166-170.
- Chen JT, Chen CH, Horng CT, et al. Glucosamine sulfate inhibits proinflammatory cytokine-induced icam-1 production in human conjunctival cells in vitro. *J Ocul Pharmacol Ther*. 2006;22(6):402-416.
- Chen JT, Chen PL, Chang YH, et al. Glucosamine sulfate inhibits leukocyte adhesion in response to cytokine stimulation of retinal pigment epithelial cells in vitro. *Exp Eye Res*. 2006;83(5):1052-1062.
- Chen JT, Liang JB, Chou CL, et al. Glucosamine sulfate inhibits TNF-alpha and IFN-gamma-induced production of ICAM-1 in human retinal pigment epithelial cells in vitro. *Invest Ophthalmol Vis Sci*. 2006;47(2):664-672.
- Aghazadeh-Habashi A, Sattari S, Pasutto F, Jamali F. Single dose pharmacokinetics and bioavailability of glucosamine in the rat. *J Pharm Pharm Sci*. 2002;5(2):181-184.
- Barnes PJ. Nuclear factor-kappa B. *Int J Biochem Cell Biol*. 1997;29(6):867-870.
- Madan B, Batra S, Ghosh B. 2'-Hydroxychalcone inhibits nuclear factor- $\kappa$ B and blocks tumor necrosis factor-alpha- and lipopolysaccharide-induced adhesion of neutrophils to human umbilical vein endothelial cells. *Mol Pharmacol*. 2000;58(3):526-534.
- Liu SF, Ye X, Malik AB. Inhibition of NF- $\kappa$ B activation by pyrrolidine dithiocarbamate prevents in vivo expression of proinflammatory genes. *Circulation*. 1999;100(12):1330-1337.
- Anderson JW, Nicolosi RJ, Borzelleca JF. Glucosamine effects in humans: a review of effects on glucose metabolism, side effects, safety considerations and efficacy. *Food Chem Toxicol*. 2005;43(2):187-201.
- Springer TA. Traffic signals for lymphocyte recirculation and leukocyte emigration: the multistep paradigm. *Cell*. 1994;76(2):301-314.
- Hubbard AK, Rothlein R. Intercellular adhesion molecule-1 (ICAM-1) expression and cell signaling cascades. *Free Radic Biol Med*. 2000;28(9):1379-1386.
- Kanagawa T, Matsuda S, Mikawa Y, et al. Role of ICAM-1 and LFA-1 in endotoxin-induced uveitis in mice. *Jpn J Ophthalmol*. 1996;40(2):174-180.
- Whitcup SM, Hikita N, Shirao M, et al. Monoclonal antibodies against CD54 (ICAM-1) and CD11a (LFA-1) prevent and inhibit endotoxin-induced uveitis. *Exp Eye Res*. 1995;60(6):597-601.
- Yang P, de Vos AF, Kijlstra A. Interferon gamma immunoreactivity in iris nerve fibres during endotoxin induced uveitis in the rat. *Br J Ophthalmol*. 1998;82(6):695-699.
- Whitcup SM, Chan CC, Li Q, Nussenblatt RB. Expression of cell adhesion molecules in posterior uveitis. *Arch Ophthalmol*. 1992;110(5):662-666.
- Grakoui A, Bromley SK, Sumen C, et al. The immunological synapse: a molecular machine controlling T cell activation. *Science*. 1999;285(5425):221-227.
- Bauerle PA, Baltimore D. NF-kappa B: ten years after. *Cell*. 1996;87(1):13-20.
- Collins T, Read MA, Neish AS, et al. Transcriptional regulation of endothelial cell adhesion molecules: NF-kappa B and cytokine-inducible enhancers. *FASEB J*. 1995;9(10):899-909.
- Sahnoun Z, Jamoussi K, Zeghal KM. [Free radicals and antioxidants: physiology, human pathology and therapeutic aspects (part II)]. *Therapie*. 1998;53(4):315-339.
- Alberts B, Johnson A, Lewis J, et al. The activation of a macrophage by LPS. In: *Molecular Biology of the Cell*. 4th ed. London: Garland Science; 2002:1458.

39. Minty A, Chalou P, Derocq JM, et al. Interleukin-13 is a new human lymphokine regulating inflammatory and immune responses. *Nature*. 1993;362(6417):248–250.
40. Doherty TM, Kastelein R, Menon S, et al. Modulation of murine macrophage function by IL-13. *J Immunol*. 1993;151(12):7151–7160.
41. Marie O, Thillaye-Goldenberg B, Naud MC, de Kozak Y. Inhibition of endotoxin-induced uveitis and potentiation of local TNF- $\alpha$  and interleukin-6 mRNA expression by interleukin-13. *Invest Ophthalmol Vis Sci*. 1999;40(10):2275–2282.
42. Cosentino G, Soprana E, Thienes CP, et al. IL-13 down-regulates CD14 expression and TNF- $\alpha$  secretion in normal human monocytes. *J Immunol*. 1995;155(6):3145–3151.
43. Di Santo E, Meazza C, Sironi M, et al. IL-13 inhibits TNF production but potentiates that of IL-6 in vivo and ex vivo in mice. *J Immunol*. 1997;159(1):379–382.
44. Lemaitre C, Thillaye-Goldenberg B, Naud MC, de Kozak Y. The effects of intraocular injection of interleukin-13 on endotoxin-induced uveitis in rats. *Invest Ophthalmol Vis Sci*. 2001;42(9):2022–2030.
45. Yang P, de Vos AF, Kijlstra A. Macrophages in the retina of normal Lewis rats and their dynamics after injection of lipopolysaccharide. *Invest Ophthalmol Vis Sci*. 1996;37(1):77–85.
46. Kamata K, Inazu M, Takeda H, et al. Effect of a selective inducible nitric oxide synthase inhibitor on intraocular nitric oxide production in endotoxin-induced uveitis rabbits: in vivo intraocular microdialysis study. *Pharmacol Res*. 2003;47(6):485–491.
47. Tilton RG, Chang K, Corbett JA, et al. Endotoxin-induced uveitis in the rat is attenuated by inhibition of nitric oxide production. *Invest Ophthalmol Vis Sci*. 1994;35(8):3278–3288.
48. Hibbs JB Jr, Taintor RR, Vavrin Z, Rachlin EM. Nitric oxide: a cytotoxic activated macrophage effector molecule. *Biochem Biophys Res Commun*. 1988;157(1):87–94.
49. Goureau O, Bellot J, Thillaye B, et al. Increased nitric oxide production in endotoxin-induced uveitis: reduction of uveitis by an inhibitor of nitric oxide synthase. *J Immunol*. 1995;154(12):6518–6523.
50. Mandai M, Yoshimura N, Yoshida M, et al. The role of nitric oxide synthase in endotoxin-induced uveitis: effects of NG-nitro L-arginine. *Invest Ophthalmol Vis Sci*. 1994;35(10):3673–3680.
51. Cao C, Matsumura K, Yamagata K, Watanabe Y. Induction by lipopolysaccharide of cyclooxygenase-2 mRNA in rat brain: its possible role in the febrile response. *Brain Res*. 1995;697(1–2):187–196.
52. Quan N, Whiteside M, Herkenham M. Cyclooxygenase 2 mRNA expression in rat brain after peripheral injection of lipopolysaccharide. *Brain Res*. 1998;802(1–2):189–197.
53. Lee SH, Soyoola E, Channugam P, et al. Selective expression of mitogen-inducible cyclooxygenase in macrophages stimulated with lipopolysaccharide. *J Biol Chem*. 1992;267(36):25934–25938.
54. Masferrer JL, Zweifel BS, Manning PT, et al. Selective inhibition of inducible cyclooxygenase 2 in vivo is antiinflammatory and non-ulcerogenic. *Proc Natl Acad Sci U S A*. 1994;91(8):3228–3232.
55. Seibert K, Zhang Y, Leahy K, et al. Pharmacological and biochemical demonstration of the role of cyclooxygenase 2 in inflammation and pain. *Proc Natl Acad Sci U S A*. 1994;91(25):12013–12017.
56. Smith JR, Hart PH, Williams KA. Basic pathogenic mechanisms operating in experimental models of acute anterior uveitis. *Immunol Cell Biol*. 1998;76(6):497–512.
57. Xie QW, Kashiwabara Y, Nathan C. Role of transcription factor NF- $\kappa$ B/Rel in induction of nitric oxide synthase. *J Biol Chem*. 1994;269(7):4705–4708.
58. Noh EJ, Ahn KS, Shin EM, et al. Inhibition of lipopolysaccharide-induced iNOS and COX-2 expression by dehydroevodiamine through suppression of NF- $\kappa$ B activation in RAW 264.7 macrophages. *Life Sci*. 2006;79(7):695–701.
59. Altman RD, Lozada CJ. Practice guidelines in the management of osteoarthritis. *Osteoarthritis Cartilage*. 1998;6(suppl A):22–24.
60. Pavelka K, Gatterova J, Gollerova V, et al. A 5-year randomized controlled, double-blind study of glycosaminoglycan polysulphuric acid complex (Rumalon) as a structure modifying therapy in osteoarthritis of the hip and knee. *Osteoarthritis Cartilage*. 2000;8(5):335–342.
61. Reginster JY, Deroisy R, Rovati LC, et al. Long-term effects of glucosamine sulphate on osteoarthritis progression: a randomised, placebo-controlled clinical trial. *Lancet*. 2001;357(9252):251–256.
62. Muller-Fassbender H, Bach GL, Haase W, et al. Glucosamine sulfate compared to ibuprofen in osteoarthritis of the knee. *Osteoarthritis Cartilage*. 1994;2(1):61–69.
63. Largo R, Alvarez-Soria MA, Diez-Ortego I, et al. Glucosamine inhibits IL-1 $\beta$ -induced NF $\kappa$ B activation in human osteoarthritic chondrocytes. *Osteoarthritis Cartilage*. 2003;11(4):290–298.
64. Shikhman AR, Kuhn K, Alaaeddine N, Lotz M. N-acetylglucosamine prevents IL-1 beta-mediated activation of human chondrocytes. *J Immunol*. 2001;166(8):5155–5160.
65. Homandberg GA, Wen C, Hui F. Agents that block fibronectin fragment-mediated cartilage damage also promote repair. *Inflamm Res*. 1997;46(11):467–471.
66. Bekesi JG, Winzler RJ. The effect of D-glucosamine on the adenine and uridine nucleotides of sarcoma 180 ascites tumor cells. *J Biol Chem*. 1969;244(20):5663–5668.
67. Monauni T, Zenti MG, Cretti A, et al. Effects of glucosamine infusion on insulin secretion and insulin action in humans. *Diabetes*. 2000;49(6):926–935.